

# STIS Echelle Observations of NGC 4151: Variable Ionization of the Intrinsic UV Absorbers<sup>1</sup>

D.M. Crenshaw<sup>2,3</sup>, S.B. Kraemer<sup>2</sup>, J.B. Hutchings<sup>4</sup>, A.C. Danks<sup>5</sup>, T.R. Gull<sup>6</sup>,  
M.E. Kaiser<sup>7</sup>, C.H. Nelson<sup>8</sup>, & D. Weistrop<sup>8</sup>

Received \_\_\_\_\_; accepted \_\_\_\_\_

Submitted to the *The Astrophysical Journal (Letters)*

---

<sup>1</sup>Based on observations made with the NASA/ESA Hubble Space Telescope. STScI is operated by the Association of Universities for Research in Astronomy, Inc. under NASA contract NAS5-26555.

<sup>2</sup>Catholic University of America and Laboratory for Astronomy and Solar Physics, NASA's Goddard Space Flight Center, Code 681, Greenbelt, MD 20771

<sup>3</sup>crenshaw@buckeye.gsfc.nasa.gov

<sup>4</sup>Dominion Astrophysical Observatory, National Research Council of Canada, 5071 W. Saanich Rd., Victoria, B.C. V8X 4M6, Canada

<sup>5</sup>Raytheon Polar Services (RPSC), NASA's Goddard Space Flight Center, Code 681, Greenbelt, MD 20771

<sup>6</sup>NASA's Goddard Space Flight Center, Laboratory for Astronomy and Solar Physics, Code 681, Greenbelt, MD 20771

<sup>7</sup>Department of Physics and Astronomy, Johns Hopkins University, Baltimore, MD 21218

<sup>8</sup>Department of Physics, University of Nevada, Las Vegas, 4505 Maryland Parkway, Las Vegas, NV 89154-4002

## ABSTRACT

We present echelle observations of the intrinsic UV absorption lines in the Seyfert galaxy NGC 4151, which were obtained with the Space Telescope Imaging Spectrograph (STIS) on the Hubble Space Telescope (*HST*) on 1999 July 19. The UV continuum flux at 1450 Å decreased by factor of about four over the previous two years and there was a corresponding dramatic increase in the column densities of the low-ionization absorption lines (e.g., Si II, Fe II, and Al II), presumably as a result of a decrease in the ionizing continuum. In addition to the absorption lines seen in previous low states, we identify a large number of Fe II absorption lines that arise from metastable levels as high as 4.1 eV above the ground state, indicating high densities ( $> 10^6 \text{ cm}^{-3}$ ). We find that the transient absorption feature in the blue wing of the broad C IV emission, seen in a Goddard High Resolution Spectrograph (*GHR*S) spectrum and thought to be a high-velocity C IV component, is actually a Si II fine-structure absorption line at a radial velocity of  $-560 \text{ km s}^{-1}$  (relative to systemic). We also demonstrate that the “satellite” emission lines of C IV found in International Ultraviolet Explorer (*IUE*) spectra are actually regions of unabsorbed continuum plus broad emission that become prominent when the UV continuum of NGC 4151 is in a low state.

*Subject headings:* galaxies: individual (NGC 4151) – galaxies: Seyfert

## 1. Introduction

NGC 4151 ( $cz = 995 \text{ km s}^{-1}$ ) is the first Seyfert galaxy known to show intrinsic absorption that could be attributed to the active nucleus. Oke and Sargent (1968) first reported evidence for nonstellar absorption from He I  $\lambda 3889$ , and Anderson & Kraft (1969) discovered H $\beta$  and H $\gamma$  self absorption. The optical absorption was blueshifted with radial velocities up to  $-970 \text{ km s}^{-1}$  with respect to the host galaxy and therefore attributed to mass ejected from the nucleus. Cromwell & Weymann (1970) discovered that the Balmer absorption is variable, and can sometimes disappear altogether.

Ultraviolet observations of NGC 4151 by the *IUE* (Boksenberg et al. 1978) and subsequent far-ultraviolet observations by the *Hopkins Ultraviolet Telescope* (*HUT*, Kriss et al. 1992) revealed a number of absorption lines from species that span a wide range in ionization potential (e.g., O I to O VI), as well as fine-structure and metastable absorption lines. The intrinsic UV absorption was found to be variable in ionic column density, but no variations in radial velocities were detected (Bromage et al. 1985). More recent observations of NGC 4151 were obtained with the Goddard High Resolution Spectrograph (GHRS) at high spectral resolution ( $\sim 15 \text{ km s}^{-1}$ ) over limited wavelength regions by Weymann et al. (1997). The GHRS spectra revealed that the C IV and Mg II absorption lines, detected in six major kinematic components, were remarkably stable over the time period 1992 – 1996. The absorption components showed no evidence for variable column or radial velocity, except that a transient feature was detected in the blue wing of the broad C IV emission in one of four GHRS observations, and was attributed to a high-velocity C IV component (Weymann et al. 1997).

In the Hubble Space Telescope (*HST*) survey of intrinsic UV absorption lines in Seyfert galaxies by Crenshaw et al. (1999), NGC 4151 stood out as an unusual object. Of the ten Seyfert galaxies in this sample with intrinsic absorption, all showed C IV and N V

absorption, but only NGC 4151 showed Mg II absorption<sup>9</sup>. NGC 4151 is also unusual in the sense that it is the only active galaxy known to show metastable C III\*  $\lambda 1175$  absorption, which is indicative of relatively high electron densities ( $\sim 10^9 \text{ cm}^{-3}$ , Bromage et al. 1985).

Due to the unusual nature of the absorption in NGC 4151, we decided to obtain STIS echelle spectra of the UV spectrum from 1150 – 3100 Å at a spectral resolution of 7 – 10 km s<sup>-1</sup> to study the intrinsic absorption in detail. These observations are part of a long-term project on NGC 4151 by members of the Instrument Definition Team (IDT) of the Space Telescope Imaging Spectrograph (STIS) on *HST*. In this letter, we concentrate on the variability of the absorption features in the spectral region surrounding the broad C IV emission. In future papers, we will present results on the entire UV spectrum, the Galactic absorption, and the kinematics and physical conditions in the intrinsic absorbers.

## 2. Observations

We observed the nucleus of NGC 4151 with the medium-resolution echelle gratings of STIS on 1999 July 19/20. Table 1 gives the details of the new observations, as well as previous STIS spectra of the nucleus in the UV that we use for comparison. The slitless G140M spectrum is discussed in Hutchings et al. (1998) and the low-resolution G140L and G230LB spectra are described by Nelson et al. (2000). We reduced the echelle spectra using the IDL software developed at NASA’s Goddard Space Flight Center for the IDT. The data reduction included a procedure to remove the background light from each order using a scattered-light model devised by Lindler (1999) rather than the standard procedure, which estimates the background from the interorder light directly. Whereas the

---

<sup>9</sup>Interestingly, a similar percentage ( $\sim 15\%$ ) of broad absorption-line (BAL) QSOs show low-ionization absorption in the form of Mg II (Weymann et al. 1991).

standard procedure resulted in significant negative fluxes (up to 10% of the continuum) for the troughs of saturated interstellar lines (such as Ly $\alpha$  and Si II  $\lambda$ 1260.4), the improved procedure brought all of these troughs close to zero (i.e., to within 1% of the continuum flux levels). For display purposes, the individual orders in each echelle spectrum were spliced together in the regions of overlap.

Figure 1 shows the C IV region for the three epochs of STIS observations that cover this region. The major kinematic components of C IV absorption identified by Weymann et al. (1997) in the GHRS spectra are labeled. These components have velocity centroids that range from  $-1575$  to  $+38$  km s $^{-1}$ , relative to the systemic redshift of  $cz = 995$  km s $^{-1}$  (from H I 21 cm observations, see de Vaucouleurs et al. 1991), and appear in all of the GHRS and STIS spectra. As noted by Weymann et al., component B originates in our galaxy and component F probably arises in the interstellar medium and/or halo of NGC 4151. There are no obvious changes in the velocity centroids or widths of the C IV components since the GHRS observations, except for a possible new broad component in the 1540 – 1547 Å region (see Kraemer et al. 2000 for more details).

It is obvious from Figure 1 that the continuum plus broad-line emission decreased considerably over the two-year period of STIS observations. The continuum flux at 1450 Å dropped by a factor of 2.3 between the last two observations (i.e., from  $2.45 \times 10^{-13}$  to  $1.06 \times 10^{-13}$  ergs s $^{-1}$  cm $^{-2}$  Å $^{-1}$  between 1998 February 10 and 1999 July 19). There are no pure continuum regions in the slitless spectrum obtained on 1997 May 25, but the continuum plus broad emission is 1.5 times higher than in 1998. Since the amplitude of continuum variations tends to be larger than that of C IV in this object (Crenshaw et al. 1996, and references therein), it is likely that the UV continuum at 1450 Å decreased by at least a factor of 1.5 from 1997 to 1998, and therefore by at least a factor of 3.5 from 1997 to 1999. This is not unusual for NGC 4151, since *IUE* observations have shown that the UV

continuum can vary by as much as a factor of 10 over a period of 2 – 3 years (Ulrich et al. 1991).

### 3. Results

#### 3.1. The Appearance of Low-Ionization Lines

Figure 1 shows an interesting change in the C IV region at the time of the STIS echelle observations, when the continuum and broad-line fluxes are low. A number of new broad (FWHM  $\approx 400$  km s $^{-1}$ ) absorption features appear in the wings of C IV which are not seen at higher states in the previous GHRS and STIS observations (with an exception discussed in Section 3.3); the strongest of these features are at the observed wavelengths of 1529 Å, 1535 Å, 1572 Å, and 1577 Å. These absorption features and others are identified in Figure 2, which gives a wider region of the spectrum near C IV. We confirm Bromage et al.’s (1985) identification of Si IV, Si II, C IV, and Al II absorption in this region, as well as their claim of resonance and fine-structure lines from multiplet UV8 of Fe II. These broad features are primarily due to component D (at a radial velocity of  $-560$  km s $^{-1}$  with respect to the host galaxy), although some lines receive a contribution from component E (at  $-255$  km s $^{-1}$ ; a full deconvolution will be given in Kraemer et al. 2000).

Many other absorption features are present in the spectrum in Figure 2. We attribute a majority of these features to Fe II multiplets that arise from metastable levels up to 4.1 eV above the ground state (Silvis & Bruhweiler 2000). As shown in Figure 2, the correspondence of the absorption features with expected positions of the Fe II lines at the radial velocity of component D is convincing. Assuming collisional excitation of the metastable Fe II levels, this implies densities of  $n_e > 10^6$  cm $^{-3}$  in this kinematic component (Wampler, Chugai, & Pettijean 1995). This is probably a severe lower limit, since densities

on the order of  $10^9 \text{ cm}^{-3}$  have been derived from the presence of metastable C III\*  $\lambda 1176$  (from a level 6.5 eV above the ground state) at this approximate radial velocity (Espey et al. 1998). A number of lines in Figure 2 remain unidentified, and we suspect that some of these may arise from higher Fe II levels (not on the lists of Fe II multiplets in Silvis and Bruhweiler). We note that the effect of all this absorption is to add structure to the UV spectrum and depress the apparent continuum and broad-line emission in many places. For example, the unusual looking feature between 1593 and 1602 Å is an unabsorbed portion of the broad wing of C IV, located between two Fe II absorption lines from multiplets 44 and EO.

### 3.2. Variable ionization of the absorption

There are two likely sources of intrinsic absorption variations in Seyfert galaxies: 1) changes in the ionization fractions due to ionizing continuum variations, and 2) changes in the total column of gas due, for example, to bulk motion of the gas across the line of sight (Crenshaw et al. 1999, and references therein). The former can be identified from a correlation between continuum and absorption variations. The best case for correlated variations has been established for the neutral hydrogen absorption and low-ionization lines of NGC 4151 on time scales of days (Kriss et al. 1996; Espey et al. 1998).

For the same Seyfert galaxy, we find strong evidence of variability in the ionization state of the absorber on longer time scales in the C IV region, where we have multiple GHRS and STIS observations at high spectral resolutions. The variation is dramatic in the sense that low-ionization lines, such as those from Si II and Fe II, are weak or undetectable when the continuum in NGC 4151 is in a high state, but are strong when the continuum drops to a low state (corresponding to  $\leq 1 \times 10^{-13} \text{ ergs s}^{-1} \text{ cm}^{-2} \text{ Å}^{-1}$  at 1450 Å). Looking back at the *IUE* observations, low states defined in this manner occurred on several occasions

over 1 – 2 year periods between 1978 and 1990 (Ulrich et al. 1991), and the published *IUE* spectra show that the low-ionization lines are strong on these occasions. This impression is supported by the finding of Bromage et al. (1985) that the equivalent widths of the low-ionization lines (e.g., Si II, Mg II) are anti-correlated with continuum flux. Thus, the appearance of low-ionization lines when the continuum reaches a low state is a long-term phenomenon, spanning at least the last two decades.

### 3.3. The transient absorption feature in GHRS spectra

The absorption feature at 1535 Å that Weymann et al. find in epoch 4 of their GHRS spectra and suggest is a “transient” C IV feature at high velocity is actually the D component of the fine-structure Si II\*  $\lambda$ 1533.4 line. This identification is firm, since the velocity centroid and full-width at half-maximum (FWHM) of this feature are essentially identical in the GHRS epoch 4 and STIS echelle spectra, and match the values determined for the D component from other lines. However, this feature is much stronger at the low continuum level of the STIS echelle spectrum (a hint of this feature can also be seen in the STIS low-resolution spectrum from 1998). The narrow absorption line in the red wing of this feature at 1537.5 Å (see Figure 1) is the E' component of Si II\*  $\lambda$ 1533.4 (at  $-210 \text{ km s}^{-1}$ ) which is identified by Weymann et al. in Mg II but not in C IV (and is also present in Si II 1526.7). Interestingly, the broad E component (at  $-255 \text{ km s}^{-1}$ ) appears to be weak or missing in the Si II\* and metastable Fe II lines, indicating a lower density for this component.

One puzzling aspect of the Si II\* absorption in the GHRS spectra is that it is seen in a relatively high state (GHRS epoch 4), similar to that of our 1997 STIS spectrum, and not seen in a lower state (GHRS epoch 2). One possible explanation is that the density of the gas responsible for this absorption is low enough that it has not had time to respond



to a previous (unobserved) continuum change. This requires the recombination time scale to be greater than or equal to the time scale for large-amplitude continuum variations, which is  $\geq 2$  days (Crenshaw et al. 1996). However, the density of the gas would have to be  $n_e \leq [\alpha_{rec} t_{rec}]^{-1} \leq [(10^{-12} \text{ cm}^{-3} \text{ s}^{-1})(1.73 \times 10^5 \text{ s})^{-1}] \leq 5.8 \times 10^6 \text{ cm}^{-3}$ , which is much lower than the derived value of  $n_e \approx 10^9 \text{ cm}^{-3}$  for the D component based on the C III\* metastable line. Another possible explanation is that the EUV and UV continuum fluxes are not well correlated, and therefore the observed UV continuum is not a good indicator of the ionizing flux (at photon energies  $\geq 16.4$  eV for Si II to Si III). We consider this possibility unlikely as well, since UV, EUV, and X-ray continuum variations appear to be correlated in this object (Edelson et al. 1996) and a number of other Seyfert galaxies (e.g., Chiang et al. 2000, Nandra et al. 2000). Thus, this issue remains open at present.

### 3.4. The C IV satellite lines

A number of *IUE* observations have shown narrow emission features in the wings of the broad C IV emission line that could not be attributed to typical Seyfert emission lines at the redshift of NGC 4151 (Ulrich et al. 1985; Clavel et al. 1987; Ulrich 1996). These lines were relatively narrow (FWHM  $\approx 7 - 16 \text{ \AA}$ ), located on either side of the C IV peak, and designated L1 and L2 at the observed positions of  $1518 \text{ \AA}$  and  $1594 \text{ \AA}$  (Clavel et al. also note a subcomponent L2' located at  $1576 \text{ \AA}$ ). These features have been identified as C IV “satellite lines” at relatively large radial velocities, and it was suggested that they may arise from a two-sided jet (Ulrich et al. 1985). Interestingly, the satellite lines were seen primarily in continuum low states, and were not detected in *HST* spectra (prior to our observations), which were obtained at moderate to bright states.

To investigate this phenomenon, we retrieved an *IUE* SWP spectrum obtained on 1983 November 19 from the *IUE* archives. This spectrum was obtained when the continuum flux

was low, and shows the satellite lines prominently (Clavel et al. 1987). Figure 3 shows the *IUE* spectrum in the C IV region, along with the STIS echelle spectrum. To compare the two spectra, we resampled the STIS spectrum to the *IUE* bin size (1.67 Å per bin) and smoothed it to the *IUE* resolution ( $\sim 5$  Å). The binned STIS spectrum is plotted as a dashed line in Figure 3.

Figure 3 demonstrates that the satellite lines (L1, L2', and L2) in the *IUE* spectra are also present in the binned STIS spectrum. In the original STIS spectrum these lines are seen to be regions of relatively unabsorbed broad-emission plus continuum in the wings of C IV, surrounded by broad low-ionization absorption lines (primarily from Si II and Fe II). The prominence of the “satellite lines” at low continuum states is therefore explained by the increased strength of the surrounding low-ionization absorption lines when the continuum flux is low.

#### 4. Conclusions

Our STIS spectra show that the broad low-ionization absorption lines appear in NGC 4151 when the UV continuum flux is low, and are therefore very sensitive to changes in the ionizing flux. This is apparently a long term phenomenon, since evidence for an anti-correlation between the equivalent widths of the low ionization lines and the UV continuum fluxes has been established for *IUE* observations dating back to 1978 (Bromage et al. 1985). High-ionization lines such as C IV are apparently close to saturation at both high and low states (with evidence for a residual flux in the troughs of these lines which is likely due to scattered light near the nucleus, see Kraemer et al. 2000).

The STIS echelle observations reveal a huge number of previously unidentified broad (FWHM  $\approx 400$  km s $^{-1}$ ) absorption features in the low-state spectrum of NGC 4151. We

identify most of these features as Fe II lines from multiplets that arise from metastable levels as high as 4.1 eV above the ground state. Although this type of absorption is rare, it has been seen in a few active galaxies and quasars with higher luminosities (e.g., Mrk 231, Smith et al. 1995; Q0059–2735, Wampler et al. 1995; Arp 102B, Halpern et al. 1996), and is indicative of low-ionization gas with at least moderate electron densities ( $n_e > 10^6 \text{ cm}^{-3}$ ).

The variability of the low-ionization lines helps to explain a couple of puzzling aspects of the UV spectrum of NGC 4151. The transient feature seen in the blue wing of the C IV emission line in GHRS spectra is actually the D component of the Si II\*  $\lambda 1533.4$  fine-structure line. The C IV “satellite lines” seen in *IUE* spectra are regions of unabsorbed continuum plus broad C IV emission that become prominent when the low-ionization absorption appears at low continuum levels. The basic nature of this absorption, however, is not well understood; future efforts will concentrate on the kinematics and physical conditions in the UV absorbers in NGC 4151.

We thank Richard Mushotzky and Fred Bruhweiler for helpful discussions and suggestions. This work was supported by NASA Guaranteed Time Observer funding to the STIS Science Team under NASA grant NAG 5-4103.

## REFERENCES

- Anderson, K.S., & Kraft, R.P. 1969, ApJ, 158, 859
- Boksenberg, A., et al. 1978, Nature, 275, 404
- Bromage, G.E., et al. 1985, MNRAS, 215, 1
- Chiang, J., et al. 2000, ApJ, 528, 292
- Clavel, J., et al. 1987, ApJ, 321, 251
- Crenshaw, D.M., Kraemer, S.B., Boggess, A., Maran, S.P., Mushotzky, R.F., & Wu, C.-C. 1999, ApJ, 516, 750
- Crenshaw, D.M., et al. 1996, ApJ, 470, 322
- Cromwell, R., & Weymann, R. 1970, ApJ, 159, L147
- de Vaucouleurs G., de Vaucouleurs A., Corwin H. G., Buta R. J., Paturel, G., & Fouque P. 1991, Third Reference Catalogue of Bright Galaxies Springer-Verlag, New York
- Edelson, R.A., et al. 1996, ApJ, 470, 364
- Espey, B.R., Kriss, G.A., Krolik, J.H., Zheng, W., Tsvetanov, Z., & Davidsen, A.F. 1998, ApJ, 500, L13
- Halpern, J.P., Eracleous, M., Filippenko, A.V., & Chen, K. 1996, ApJ, 464, 704
- Hutchings, J.B., Crenshaw, D.M., Kaiser, M.E., Kraemer, S.B., Weistrop, D., Baum, S., Bowers, C.W., Feinberg, L.D., Green, R.F., Gull, T.R., Hartig, G.F., Hill, G., and Lindler, D.J. 1998, ApJ, 492, L115.
- Kraemer, S.B., et al. 2000, in preparation
- Kriss, G.A., et al. 1992, ApJ, 392, 485
- Kriss, G., Krolik, J., Grimes, J., Tsvetanov, Z., Zheng, W., & Davidsen, A. 1996, in proc. IAU Colloquium 159, Emission Lines in Active Galaxies: New Methods and

- Techniques, eds. B.M. Peterson, F.-Z. Cheng, & A.S. Wilson (Astronomical Society of the Pacific: San Francisco), 113, 453.
- Lindler, D. 1999, CALSTIS Reference Guide (CALSTIS Version 6.4)
- Nandra, K., et al. 2000, ApJ, in press
- Nelson, C.H., Weistrop, D., Hutchings, J.B., Crenshaw, D.M., Gull, T.R., Kaiser, M.E., Kraemer, S.B., & Lindler, D. 2000, ApJ, 531, 257
- Oke, J.B., & Sargent, W.L.W. 1968, ApJ, 151, 807
- Silvis, J.M. & Bruhweiler, F.C. 2000, in preparation
- Smith, P.S., Schmidt, G.D., Allen, R.G., & Angel, J.R.P. 1995, ApJ, 444, 146
- Ulrich, M.-H. 1996, MNRAS, 281, 907
- Ulrich, M.-H., et al. 1985, Nature, 313, 747
- Ulrich, M.-H., et al. 1991, ApJ, 382, 483
- Wampler, E.J., Chugai, N.N., & Petitjean, P. 1995, ApJ, 443, 586
- Weymann, R.J., Foltz, C.B., & Hewett, P.C. 1991, ApJ, 373, 23
- Weymann, R.J., Morris, S.L., Gray, M.E., & Hutchings, J.B. 1997, ApJ, 483, 717

Fig. 1.— STIS spectra of the nucleus of NGC 4151 in the C IV region at three epochs. The low-resolution spectrum from 1998 is plotted as a dashed line. The positions of the major kinematic components of absorption from Weymann et al. (1997) are given in capital letters for the C IV  $\lambda 1548.2$  line and small letters for the C IV  $\lambda 1550.8$  line.

Fig. 2.— Identification of the broad absorption lines in the 1350 – 1700 Å region; vertical lines represent the locations of the D component (at  $-560 \text{ km s}^{-1}$ , with respect to systemic). Fe II multiplets in this region are plotted below the spectrum, with the length of the vertical lines representing the strength of the  $gf$  values; multiplets that have at least one line with  $\log(gf) > -0.7$  from the lists of Silvis & Bruhweiler (2000) are plotted.

Fig. 3.— Comparison of STIS and IUE spectra for NGC 4151 at low continuum states. The original STIS spectrum is offset in flux by  $2.0 \times 10^{-13} \text{ ergs s}^{-1} \text{ cm}^{-2} \text{ \AA}^{-1}$  and the binned STIS spectrum is offset by  $0.5 \times 10^{-13} \text{ ergs s}^{-1} \text{ cm}^{-2} \text{ \AA}^{-1}$ . The locations of emission lines and the “satellite lines” are given.

Table 1. STIS UV Observations of the Nucleus of NGC 4151

Date (UT)	Grating	Aperture	Exp. Time (sec)	Coverage (Å)	Resolution (km s <sup>-1</sup> )
Echelle Spectra					
1999 July 19/20	E140M	0".2 x 0".2	5546	1146 – 1710	7
	E230M	0".2 x 0".2	2632	1614 – 2360	10
	E230M	0".2 x 0".2	2304	2278 – 3092	10
Previous STIS Spectra					
1997 May 25	G140M	25" x 25"	2369	1522 – 1576	20
1998 January 8	G230LB	25" x 0".2	2160	1680 – 3060	300
1998 February 10	G140L	25" x 0".2	4500	1150 – 1730	240

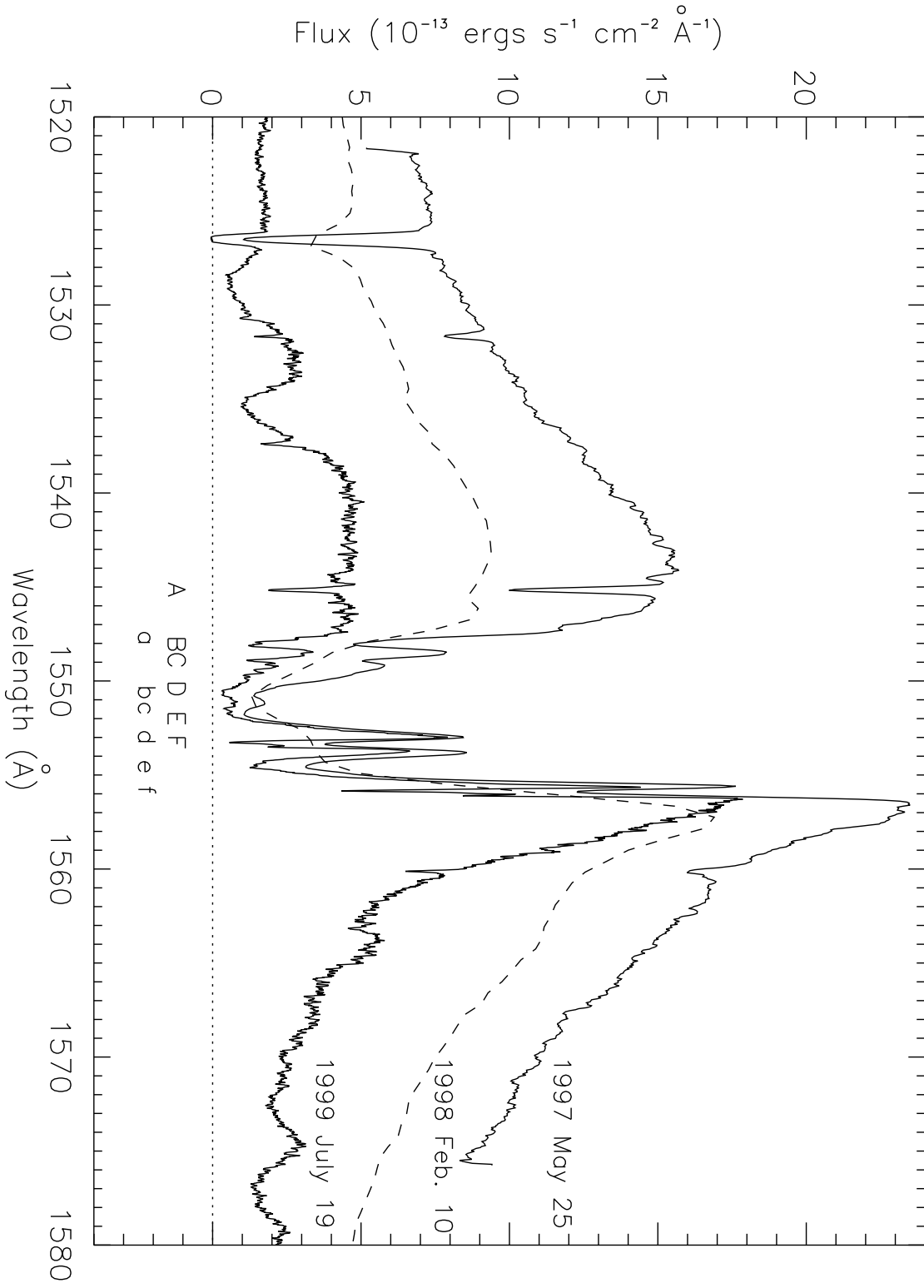


Fig. 1.



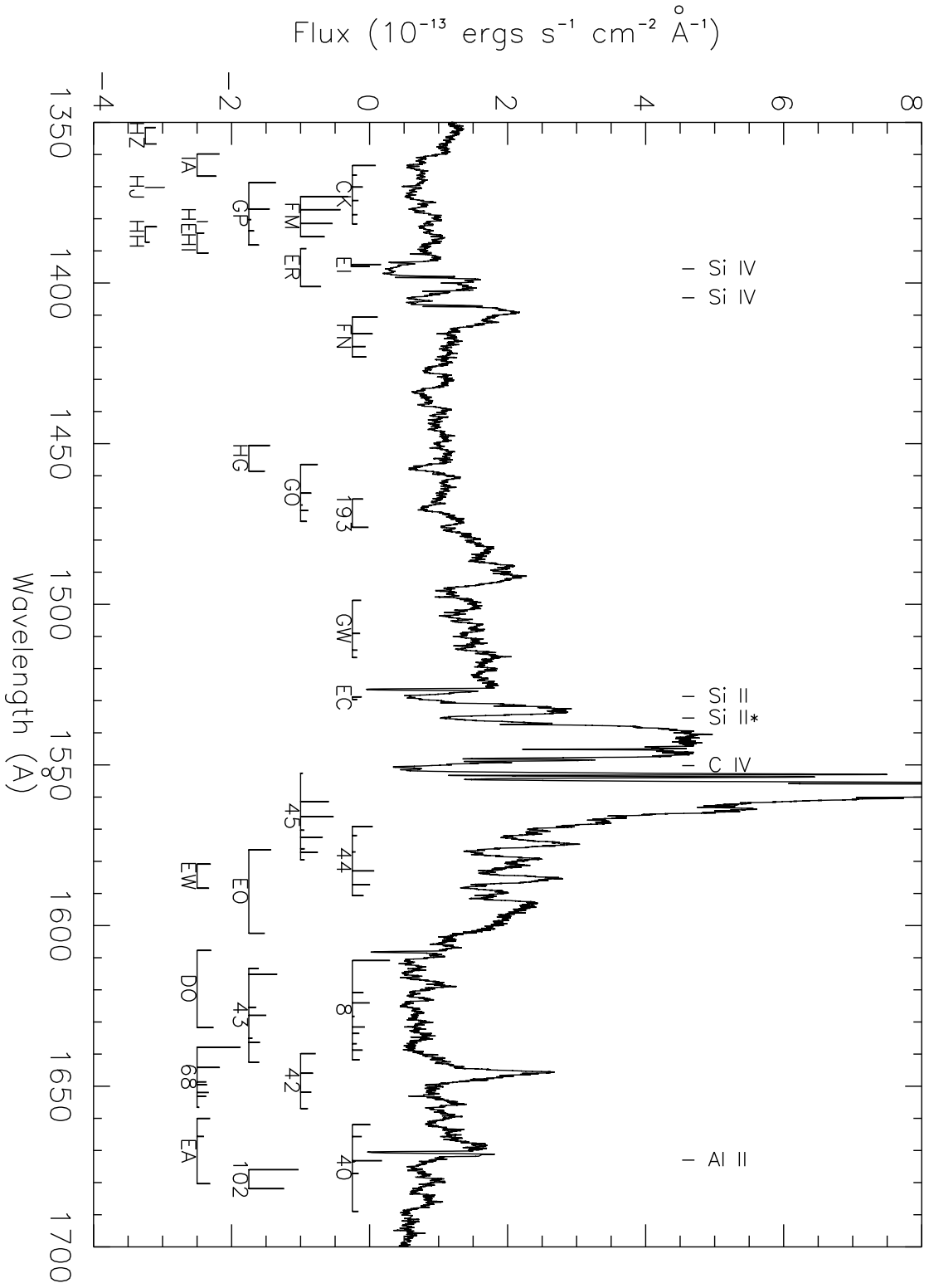


Fig. 2.

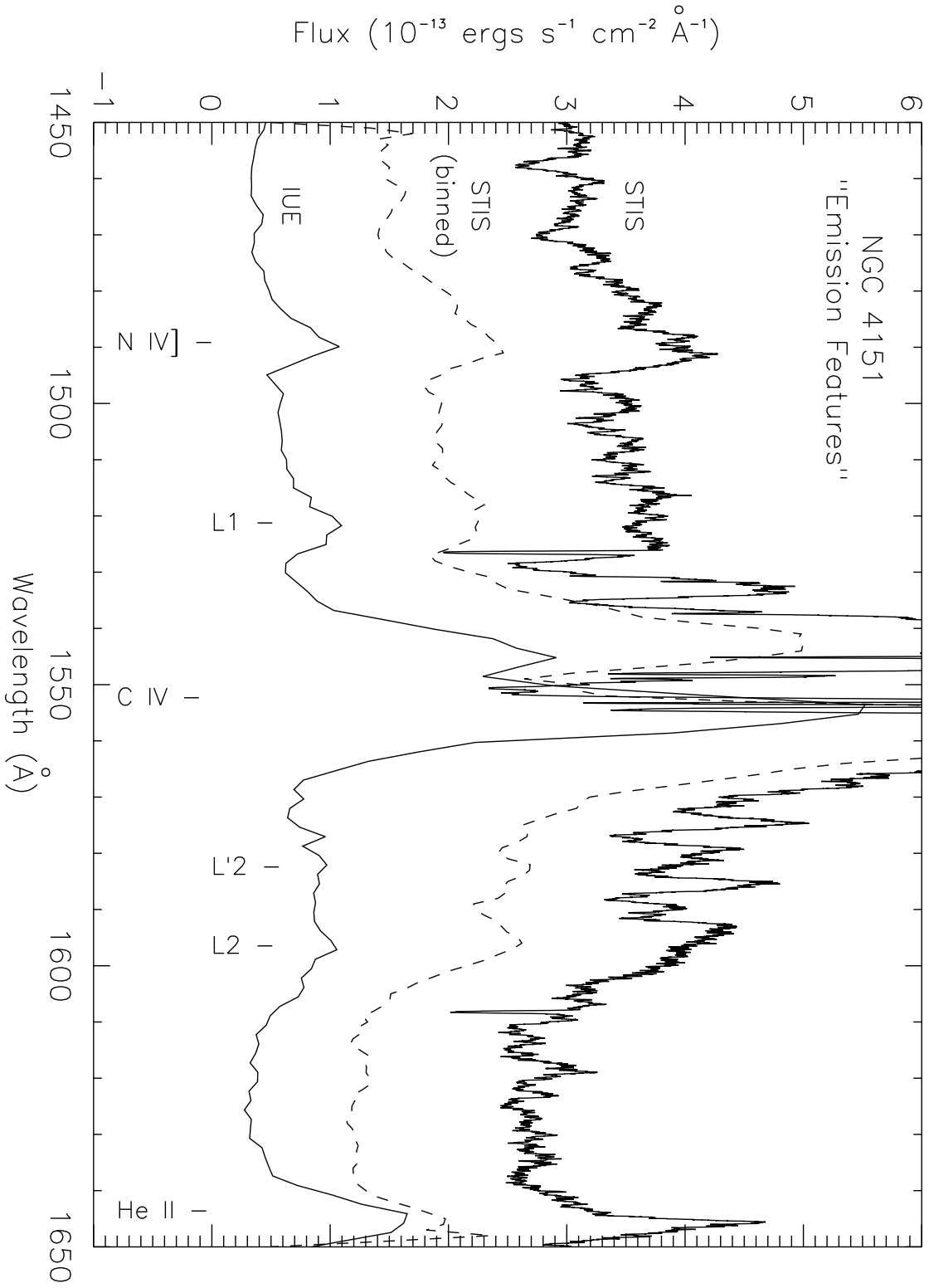


Fig. 3.